Journal of Materials Chemistry B

Accepted Manuscript

ROYAL SOCIETY OF CHEMISTRY

www.rsc.org/materialsB

Journal Name

RSCPublishing

ARTICLE

Amino- and ionic liquid-functionalised nanocrystalline ZnO via silane anchoring - an antimicrobial synergy

Cite this: DOI: 10.1039/xoxxoooooox

Received ooth January 2012,
Accepted ooth January 2012

DOI: 10.1039/xoxxoooooox

www.rsc.org/

Marjeta Čepin[a], Vasko Jovanovski[a*], Matejka Podlogar[b] and Zorica Crnjak Orel[a*]

The synthesis of highly antimicrobial nanocrystalline zinc oxide and its covalent modifications is presented. In order to achieve further improvement of antimicrobial activity, surface of ZnO was effectively modified with selected silanes comprising amino- and ionic liquid-functionalities. We demonstrate for the first time ionic liquid surface immobilization on ZnO and application of this hybrid material for antimicrobial purposes. Different microscopic and spectroscopic techniques as well as size, surface and elemental composition analysis were employed to prove these modifications. Characterisations revealed that surface and antimicrobial properties strongly depend on the modification employed. Most of the amino- and ionic liquid-functionalised nanocrystalline ZnO exhibited improved antimicrobial activity compared to commercially available silane-containing antimicrobial agent attached to nanocrystalline ZnO. Bacterial growth reduction was assessed by following optical density of bacterial growth with different concentrations of the novel antimicrobial nanomaterials. Complete bacterial inactivation was achieved for specific amino- and ionic liquid-modifications at 0.125 g L^{-1}, revealing synergistic effect of ZnO and its modifications, exhibiting up to 2-fold improvement compared to unmodified ZnO.

Introduction

Zinc oxide (ZnO) nanostructures are gaining increasing interest in numerous areas of material research. This abundant and non-toxic metal oxide is widely used as a semiconductor in design of photocatalysts[1,2], solar cells[3,4], gas and chemical sensors[5,6], catalysts[7], piezoelectric transducers[8], opto-electrical devices[9], UV shielding[10] and bioimaging[11]. In addition, ZnO is used in antifouling paints[12] and for water disinfection and microbial control[13]. For this wide range of applications ZnO is often used in the form of particles and the size and surface properties of the these are of great importance.

Adsorbed or more attractive covalently bonded organic layers onto the surface of metal oxides[14] have been widely researched and can be used to alter surface properties to serve numerous applications. Functionalizations of metal oxides in particular, could be beneficial because of the importance of these materials in several hybrid inorganic-organic applications. For this purpose, functional trialkoxysilane anchoring compounds have often been used as they form covalent bonds with both inorganic and organic materials. Hitherto reported silane functionalization was mainly focused on silica nanoparticles, TiO_2, ZnO and others for obtaining promising hybrid systems. They are currently investigated for use in biosensors[15], light-emitting diodes[16] and polymers with tailored properties[17]. Another practical aspect of surface modification is to prevent agglomeration[18] of metal oxides and growth of nanostructures[19] by reducing surface energy. Various ZnO structures with modified surface have been thus far employed for electrochemically adjustable wettability by using ferrocene-functionalised silane[20], tailoring wetting behaviour[21-23], grafting PMMA onto ZnO particles[18,24], biotinylation of ZnO nanoparticles[25], and solid-phase extraction[26] by using long-chain alkyltrimethoxysilane.

Ionic liquids are a well-established family of materials known for their extraordinary chemical and physical properties, e.g. liquid at temperatures below 100 °C, negligible vapour pressure, high ionic and temperature conductivity, and they have found way into numerous applications, e.g. optoelectronic devices[27,28], batteries[29], supercapacitors[30], polymers[31], bio-applications[32] etc. Ionic liquids have been also employed in ZnO synthesis[33-36], however to our best knowledge ionic liquids have never been chemically grafted onto ZnO surface.

Ionic liquids are close relatives of quaternary amines that have been used extensively and very effectively by Klibanov et al. as

antimicrobial agents[37, 38], efficiently rupturing cell membranes on contact with no developed resistance[39]. Development of antimicrobial materials is a fast-growing field[40] especially with the focus on preparing antibacterial coatings for prevention of spreading infections, particularly non-selective robust antimicrobial agents such as metal oxides[41]. ZnO in its various morphologies and its composites possesses good antimicrobial properties[13, 42-46] exhibited even in the absence of UV illumination against bacteria[43, 47] and fungi[44]. It has also been reported to be a superior antibacterial agent compared to the more commonly studied TiO_2[43]. Its effectiveness and robustness make it very attractive for practical applications. There are different hypotheses about the mechanism of ZnO's antibacterial action. Commonly accepted mechanism is formation of reactive oxygen species (H_2O_2, $HO^{\cdot}$, O_2^{-})[48], predominantly under UV illumination, causing oxidative stress on bacterial membrane. Release of Zn^{2+} can also contribute to the toxicity of ZnO[13] and was even proposed to be a dominant mechanism of toxicity of ZnO[49]. There are also reports proving ZnO nanoparticle surface itself triggering fatal bacterial membrane disorganization on contact even without significant release of Zn^{2+} [50]. Few reports also claim bacterial growth inhibition due to accumulation of ZnO nanoparticles in cytoplasm[50, 51].

Since all of the abovementioned mechanisms involve the active surface of ZnO, further improvement of the antimicrobial activity would be achieved by surface modification. Antibacterial studies have been mainly performed on the bare ZnO nanomaterials, scarcely on the surface-functionalized nanomaterials[47,51-53], although it has been shown that the functionalised surface can significantly affect antimicrobial activity of ZnO, as well as other materials such as TiO_2[54].

In this work we focused on the synthesis of nanocrystalline ZnO with very high inherent antimicrobial activity and development of a simple method for their functionalization with selected amino and ionic liquid-functionalised silane anchoring groups to obtain novel hybrid materials that even further enhance the antimicrobial efficiency against Gram-negative bacteria *Escherichia coli* (*E. coli*) and Gram-positive *Staphylococcus aureus* (*S. aureus*). Silanes with one, two and three amino groups were chosen for the task as well as two ionic liquid silanes. This is the first example of using ionic liquid surface modification for antimicrobial applications to our best knowledge. Surface modifications for antimicrobial study were compared with pristine ZnO and ZnO modified with a surface agent commonly used due to its strong antimicrobial properties.

A comprehensive structural and antimicrobial characterization of produced ZnO nanocrystals was performed. Ionic liquid and some amines immobilisation on the surface of nanocrystalline ZnO were studied and its significant increase the antimicrobial activity will be presented and discussed.

Experimental section

Zinc nitrate hexahydrate ($Zn(NO_3)_2 \cdot 6H_2O$, Sigma-Aldrich), sodium hydroxide (NaOH, Merck), ethylene glycol (EG, Merck), 3-Aminopropyltrimethoxysilane (ABCR), N-(2-aminoethyl)-3-aminopropyltrimethoxysilane, 3-methoxysilylpropyldietilenetriamine, bis-(trimethoxysilylpropil)amine (ABCR), octadecyldimethyl(3-trimethoxysilylpropyl) ammonium chloride (60 % in methanol, ABCR), 3-chloropropyltrimethoxysilane (ABCR), 1-methylimidazole (ABCR), 3-methylpyridine (ABCR), toluene (Aldrich), diethylether (Aldrich) and etanol (EtOH, absolute and 96%, Carlo Erba) were of analytical grade and were used without further purification. Luria-Bertani broth (LB) bacteria growth medium was prepared by standard procedure described in ref.[55].

Nanocrystalline ZnO was prepared by solvothermal synthesis following a slightly modified procedure reported in the work of Ghoshal et al.[56]. 0.2 M $Zn(NO_3)_2$ and 0.2 M NaOH were mixed in EG/water (volume ratio of 1:1), keeping the total concentration of zinc ions and sodium hydroxide in the 800 mL reaction mixture constant at 0.1 M. Synthesis of ZnO was carried out in a sealed laboratory Teflon bottle (capacity 1 L) at 90 °C for 2 h. Soluble by-products were removed by repetitive centrifugation (6 min at 8.000 rpm min^{-1}) and washing with water and the obtained white precipitate was dried in an oven at 60 °C for 12 h.

1-Methyl-3-[3-(trimethoxysilyl)propyl]imidazolium chloride (IL1') was synthesised according to our previously published procedure[57,58] but using chloro-derivatised silane instead. 37.2 g (0.19 mol) 3-chloropropyltrimethoxysilane was added to a solution of 1-methylimidazole 14.6 g (0.18 mol) in 100 mL toluene. The mixture was refluxed for 16 h resulting in formation of two phases. The mixture was allowed to cool and the solvent was decanted. Crude ionic liquid was transferred to a separatory funnel, washed three times with 100 mL of diethylether and dried in vacuo. 37.1 g (74 %) of yellowish liquid MTMSPIC was obtained. ^{1}H NMR (400 MHz, DMSO-d_6, δ): 0.55 (m, 2H), 1.82 (broad s, 2H), 3.4 (s, 9H), 3.9 (s, 3H), 4.2 (m, 2H), 7.7 (s, 1H), 7.8 (s, 1H), 9.2 (t, J =7.7 Hz, 1H).

3-Methyl-1-[3-(trimethoxysilyl)propyl]pyridinium chloride (IL2') was synthesised in a similar manner, which also corresponds with the procedure described in ref.[59]. 35.3 g (0.18 mol) 3-chloropropyltrimethoxysilane was added to a solution of 3-methylpyridine 15.7 g (0.17 mol) in 100 mL toluene. The mixture was refluxed for 16 h after which two phases formed. The mixture was allowed to cool which resulted in precipitation of the product. Crude ionic liquid was filtered under reduced pressure, washed several times with 100 mL diethylether and dried. 31.2 g (62 %) of hygroscopic white solid MTMSPIC was obtained. ^{1}H NMR (400 MHz, DMSO-d_6, δ): 0.6 (m, 2H), 2.0 (m, 2H), 3.16 (s, 3H), 3.48 (s, 9H), 4.63 (m, 2H), 8.09 (dd, 1H, J_1=8 Hz, J_2=6 Hz), 8.50 (dd, 1H, J_1=8 Hz, J_2=0.6 Hz), 9.12 (m, 1H), 9.25 (s, 1H).

Functionalization of the nanocrystalline ZnO

In a typical experiment 0.5 g of prepared ZnO was dispersed in 40 mL ethanol (96 %) together with 2 mL of silane in a round-bottom flask and sonicated for 15 minutes. After, the flask was transferred to a heating mantle and refluxed under nitrogen for 24 h. After cooling the functionalised ZnO was collected by centrifugation followed by copious washings with ethanol and drying at 60 °C for 16 h.

The samples were characterized by scanning field emission electron microscopy (FE-SEM, Zeiss Supra 35 VP) in order to define their size and morphology. For FE-SEM measurement, materials were first sonicated and filtered through 200 nm filter paper (Millipore) previously sputtered with gold.

Samples were further studied using TEM microscope (JEM 2100, Jeol Ltd., Tokyo, Japan) operating at 200 kV. A fraction of the particles in the form of a suspension in ethanol was transferred on a lacy, carbon-coated Cu-mesh, dried and examined with the microscope. High-resolution TEM (HRTEM) and Fourier transform (FFT) pattern were employed in order to examine the structure of the materials.

X-Ray powder diffraction analyses (XRD) were carried out on a Siemens D5000 X-ray diffractometer with Cu-Kα radiation (λ = 1.54 Å) at 40 kV and 30 mA.

Infrared spectra of pristine and functionalized ZnO nanocrystals were recorded on a Bruker model IFS 66/S equipped with an attenuated total reflection (ATR) cell (SpectraTech) with a diamond crystal (n = 2.4). The spectra were recorded over the range 4000 – 370 cm^{-1}, with a resolution of 4 cm^{-1} and averaged over 128 spectra.

For size distribution measurements dynamic light scattering (DLS) was performed using a Zetasizer Nano ZS laser scattering system with a 633 nm laser source (Malvern Instruments, UK). The intensity of scattering light was maintained at 173° to minimize the effect of multiple scattering. Setting of measurement material refractive index was 2.00. The investigated water suspensions were put into 10 mm diameter polystyrene cuvettes (Brand, Germany). All analyses were run at 25 °C in 20 repetitions.

Zeta potential measurements were carried out in a Malvern Zetasizer Nano Series (Malvern Instruments, UK). Bare and modified ZnO nanocrystals were suspended in MQ water and sonicated. The average of the zeta potential values was calculated by three independent measurements. pH of the measuring solutions was kept at 8.0.

Elemental analysis was performed with an inductively coupled plasma atomic emission spectrometer (ICP-AES) (Thermo). Bare and modified ZnO nanocrystals were dissolved in 5 % HCl solution and analysed for Zn and Si content in the samples. For determination of solubility of Zn^{2+} and corresponding silanes 10 mg of the examined material were mixed with 10 mL of LB medium. The samples were stirred at 37 °C for 12 h simulating the conditions of bacterial growth analysis.

The antibacterial activity of zinc oxide nanoparticles was measured in antibacterial assay using microtiter plates for bacterial growth.

Gram-negative bacteria *E. coli* strain DH5α and Gram-positive *S. aureus* were used to test growth inhibition studies of ZnO nanoparticles. For antibacterial assay, the bacterial strain was first grown on solid nutrient agar medium and from the agar 20 mL LB medium was inoculated with fresh bacterial colony and incubated at 37 °C overnight in an Erlenmeyer flask with vigorous shaking at 170 rpm. Then 500-fold dilution of the overnight culture was made and incubated until the culture reached exponential phase. Working cell solutions were prepared with optical density 0.01 at 600 nm (OD_{600}). OD_{600} of 0.5 corresponded to a concentration of $4x10^8$ CFU mL^{-1} of medium.

All ZnO sample suspensions were prepared prior to the experiments in sterile MQ water to a stock solution of 40 mg mL^{-1} and all samples were sonicated for 15 min at 40 kHz. Stock suspensions were diluted to the required final concentrations in LB medium.

To examine the bacterial growth rate or the bacterial growth behaviour in the presence of pristine and functionalised ZnO nanocrystals, bacterial cells were grown in a 96-well microtiter plate containing LB medium supplemented with various concentrations of ZnO. Serial dilutions of suspensions in a volume of 200 µL were pipetted onto microtiter plate. Final ZnO concentrations were as follows: 0.5, 0.25, 0.125 and 0.0625 mg mL^{-1}. Each plate had samples in triplicates and a set of controls: ZnO in LB medium as a blank value for OD_{600} measurements and inoculated medium without ZnO. Similar experiments were performed also for Zn^{2+} and examined silanes $Zn(NO_3)_2 \cdot 6\ H_2O$ was taken as Zn^{2+} source.

The bacterial growth curves were acquired by measuring OD_{600} of the cultures and plotting it against time. OD measurements were made using Synergy 4 Multi-Mode Microplate Reader (BioTek) controlled by Gen5™ Software. Cells were shaken in a microplate reader at 37 °C and measurements were made every 10 minutes for 15 hours. Reusability study was performed by adding fresh inoculums of E. coli every 12 h for 5 days.

Plate assay method was used to determine the presence of viable bacteria by plating *E. coli* after 12 h treatment onto LB agar plates containing 0.5 and 0.25 g L^{-1} of ZnO-based materials and incubated at 37 °C. Confocal laser scanning microscope (Leica TSP SP5) was employed after treatment with 0.125 g L^{-1} of investigated ZnO materials using the same conditions as for plate test to determine Live/Dead assay with L7012 LIVE/DEAD *Bac*Light™ Bacterial viability kit (Molecular probes). *E. coli* was labelled with green SYTO (live and dead bacteria) and red propidium iodide (only dead bacteria) dyes. Growth media (LB) was replaced with 0.85 % NaCl aqueous solution. 1 µL of solution containing equal volumes of both dyes was added to bacterial suspensions and after 15 minutes in the dark measured with the microscope. Where no or little surviving bacteria were observed, more concentrated bacterial suspension was taken for measurements.

Statistical analysis

For both bacterial strains growth curves were fitted (non-linear regression) to the Sigmoidal-Boltzmann equation with Origin software:

$$OD_{600} = \frac{OD_I - OD_F}{1+e^{(t-t_0)/dt}} + OD_F \qquad \text{Eq. 1}$$

where OD_I is the estimated initial optical density, OD_F is the measured final OD and t_0 is the centre (where OD takes on the average of OD_I and OD_F). The curves were fitted individually and the results (average OD, standard deviation and minimal inhibitory concentration (MIC) for 90 % of bacterial growth inhibition) were taken after 12 h.
Bacterial growth reduction was calculated from fitted growth curves for modified materials after 12 h following the equation[60]:

$$R,\% = \frac{OD_{control} - OD_{sample}}{OD_{control}} \times 100\% \qquad \text{Eq. 2}$$

where $OD_{control}$ and OD_{sample} are optical density measured for the control sample (without antimicrobial agents) and the nanocrystalline ZnO materials, respectively.

Results and discussion

It has been observed that different morphologies of ZnO nanomaterials have diverse effects on antimicrobial capacity[51]. There are several reports of using colloidal ZnO suspensions, exhibiting high crystallinity or even ZnO quantum dots, as exceptionally effective antimicrobial agents[43,51,61-63]. Therefore, our goal was to prepare nanocrystalline ZnO with high inherent antimicrobial activity before any further surface modification. Out of several synthetic approaches towards ZnO nanomaterials from our past work[64-66] (not shown) we opted for synthesis of ZnO nanocrystals following modified procedure presented in the work of Ghoshal et al.[56]. Namely, the ethyleneglycol/water solvent mixture afforded sufficient conditions to effectively produce highly nanocrystalline ZnO at rather low temperature (90 °C, 2 h) in favourable yields (45 %).

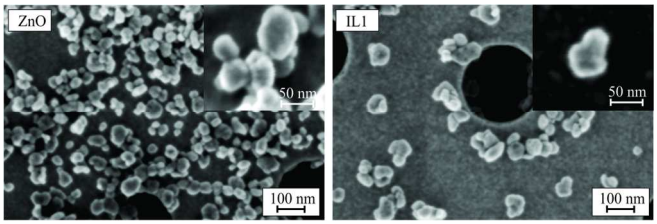

***Figure 1**: SEM images of prepared untreated ZnO nanocrystals (left) and ZnO functionalised with **IL1** ionic liquid modification (right).*

SEM microscopy showed well-separated particles of ZnO with size ≤ 50 nm (Figure 1). XRD analysis unveiled wurtzite-type ZnO (JCPDS 01-089-1397, Figure 2). According to the Debye-Scherer's equation from XRD pattern the size of ZnO crystallites was determined to be about 30 nm. Characterization of the synthesized ZnO using TEM confirmed the high crystallinity of the powder (Figure 3b, 3c, FFT pattern). This high resolution image also reveals how the crystal lattice abruptly ends and it is free of any amorphous layer. As-prepared ZnO had comparable or even enhanced antimicrobial activity (Table 1) compared to other reported ZnO nanomaterials[51,61-63]. It should be stressed that all the antimicrobial measurements were done without prior illumination of the samples; therefore any photocatalytic effect of ZnO should be excluded. Since amines, especially quaternary ones have proven to be very efficient antimicrobial materials and there have been some cases of using aminopropyltrimethoxysilane in combination with ZnO, we expanded the study by employing silanes having additional amino groups. The goal was to examine the contribution of also secondary amines to the overall antimicrobial activity. Ionic liquids can also be considered to some extent as quaternary amines with heterocyclic aromatic cations. Since they have never been used for this application two ionic liquids were designed to comprise a silane anchoring group with imidazolium and pyridinium cation, respectively.

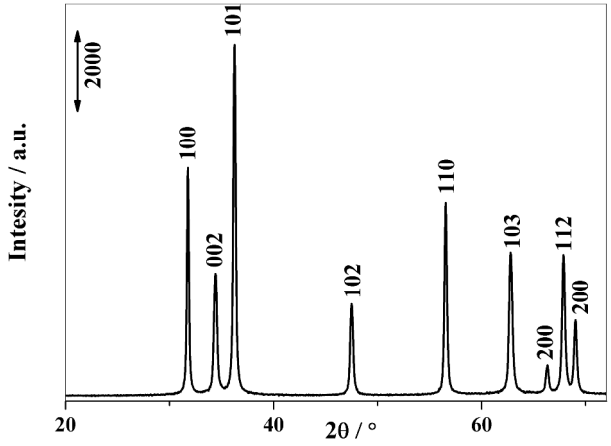

***Figure 2**: XRD diffractogram of untreated (pristine) ZnO nanocrystals.*

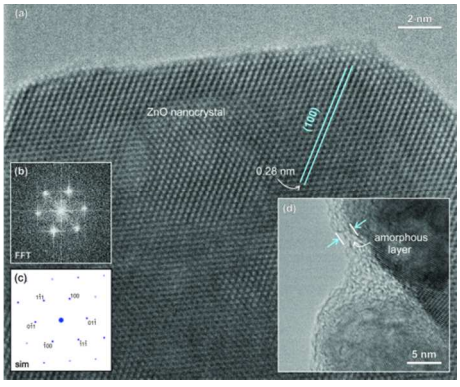

***Figure 3**: (a) TEM image of untreated ZnO nanocrystal in the (011) direction showing a lattice distance in (100) plane. (b) Corresponding fast Fourier transform (FFT) pattern along with (c) simulated diffraction pattern. (d) TEM image of ZnO covered with amorphous layer of IL1.*

It is well-known that quaternary amines exhibit high antimicrobial activity with positive charge attracting the slightly negative charged bacterial membrane and a long alkyl chain pendant group rupturing the cell membrane. However, it was shown that simple aminopropyltrimethoxysilane exhibited good antimicrobial efficacy[39,53]. Probably positive charge originating from protonation of amino group at pH 7 (pKa of $-NH_3^+ \approx 9$) is sufficient for rupturing the cell membrane in the absence of long alkyl chain. Therefore, more amino groups would further contribute to the overall positive charge and hence antimicrobial activity unless a longer amino-containing chain would manifest sterical constrains for effective binding to the ZnO surface. In this case only a partial surface coverage would occur, hindering full antimicrobial potential of the surface modification. On the other hand a fully-covered ZnO surface with a modification having poor antimicrobial activity would prevent either the ZnO surface or released Zn^{2+} to come in contact with the bacteria membrane. Semipermeable coverage would therefore display the synergy of both ZnO and its surface modification.

Surface modification of nanocrystalline ZnO with amino and ionic liquid groups via silane anchoring is shown in Scheme 1. All reactions were carried out in 96 % ethanolic (4 % water) solution under reflux temperature which proved the most optimal regarding homogeneity out of several solvents investigated, such as toluene or tetrahydrofurane (not shown). A large excess of amine served as alkaline catalyst for condensation of silane onto ZnO surface.

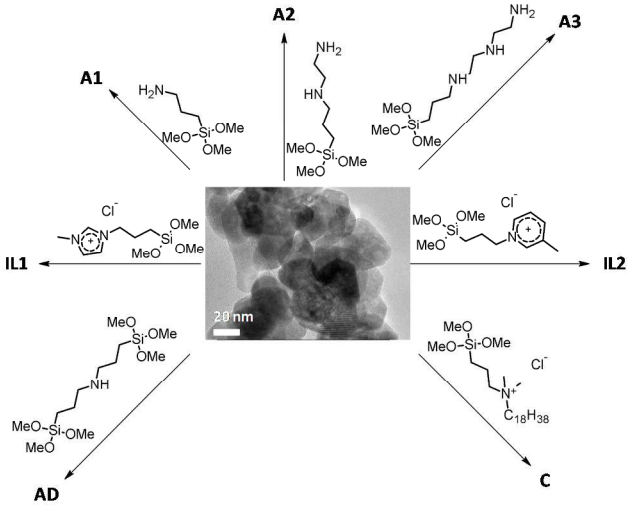

***Scheme 1**: Modification of nanocrystalline ZnO with different amino and ionic liquid functionalities via silane anchoring.*

Several experiments were performed to prove successful functionalization of ZnO. SEM images (Figures 1 and 4) of modified ZnO nanocrystals show nearly no difference in size and shape of the particles, however depending on the certain modification, agglomeration of particles became more evident. Modifications **A2**, **A3**, **IL1**, **IL2** exhibit even more improved separation of particles compared to pristine ZnO. Modification **AD** unveiled strong agglomeration as a consequence of covalent association between double-silane and ZnO. **C**-modification revealed moderate agglomeration as a result of intermolecular dispersive forces between long alkyl chains. **A1**-modification showed some particle agglomeration, probably due to short length of the aminopropyl group. These results are in accordance with the DLS and ζ-potential measurements discussed further below. DLS measurements further confirmed the increased sizes of particles in suspensions (listed in Table 1) due to the measured hydrodynamic diameter. In the case when bis-(trimethoxysilylpropil)amine (**AD**) was used the two silane groups caused substantial agglomeration of particles. HR-TEM image of **IL1**-modification revealed approximately a 2 nm amorphous layer not present in unmodified ZnO presented as inset in Figure 3d. Infrared analysis depicted in Figure 5 revealed characteristic bands for C-H stretching in the 2994-2800 cm^{-1} region. Logically, this band was more intense with modifications having longer alkyl chains. Strong bands ascribed

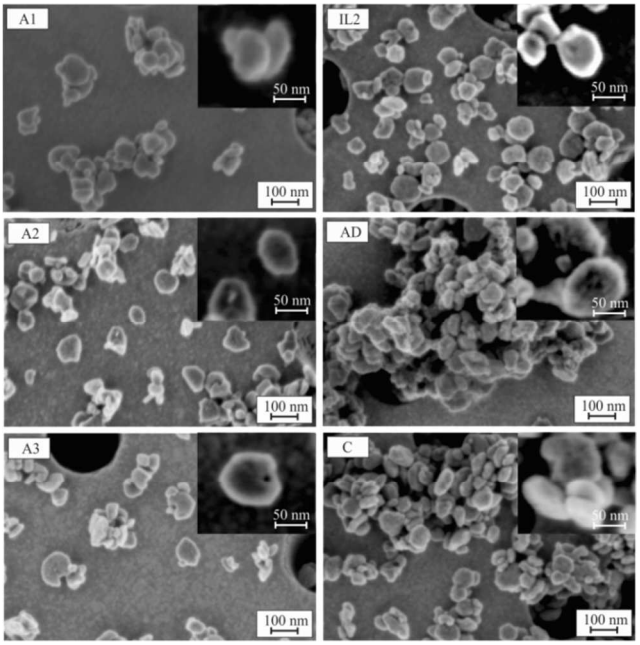

***Figure 4**: SEM images of different modifications of ZnO nanocrystals. Inset images at higher magnification.*

to Si-O-Si at 1013 and 1100 cm^{-1} appeared only with previously mentioned **AD** showing preferential silane-silane condensation. Other silanes exhibited only a weak shoulder in this region of the IR spectrum proving successful surface modification of ZnO associated with the broad band at 750-900 cm^{-1}, probably a consequence of overlaying of Si-O-Zn, Si-C and Si-O-Si bands[67]. IR spectra in this region unveiled significantly increased intensity of this band compared to the pristine ZnO. Additionally, broad absorption bands at 3370 cm^{-1} and 1640 cm^{-1} were respectively assigned to the stretching and bending vibration modes of -OH groups on the surface of ZnO[18]. The broad band in the region from 1500 to 1270 cm^{-1} was attributed to various modes of nitrate (1390 cm^{-1})[68], A-type band at 1275 cm^{-1} ($-NH_2$) and methyl and methylene deformations (1480-

1280 cm^{-1})[69]. A very strong band at 485 cm^{-1} indicated two transverse optical stretching modes of ZnO[18].

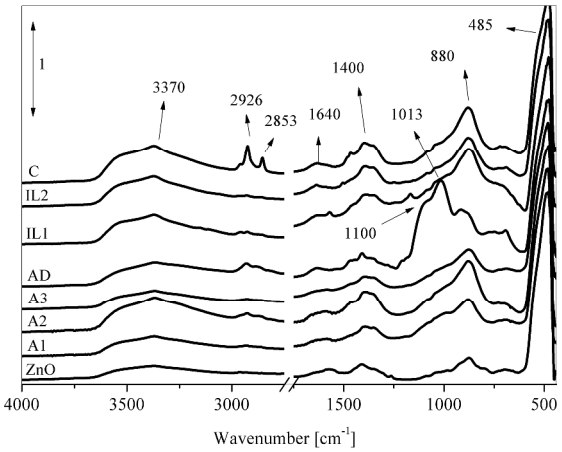

***Figure 5**: Infrared spectra of pristine and functionalized ZnO nanocrystals.*

To corroborate the surface modification ζ-potential measurements were performed. The results gathered in Table 1 show significant surface alteration as values stretched from -37 mV for unmodified ZnO (which corresponds with the value previously reported[70]) to above 30 mV for some aminosilane and ionic liquid modifications. Aminopropyltrimethoxysilane (**A1**), bis-(trimethoxysilylpropil)amine (**AD**) and octadecyldimethyl(3-trimethoxysilylpropyl) ammonium chloride (**C**)-modified ZnO revealed 5.1 mV, 6.7 mV and 5.5 mV values, respectively. Low value of **A1**-modification can be explained with short alkyl chain length allowing some amino groups to turn towards ZnO acting as ligands. **AD** exhibits predominantly siloxane character and agglomerated the particles, which both contributed to lower ζ-potential values. **C**-surface functionalization also increased the size of particles (DLS) and gave them a hydrophobic and non-ionic character. In addition, very long alkyl chains enabled intermolecular dispersive forces to prevail making such modified ZnO very unstable in suspension. In case of 3-methoxysilylpropyldietilenetriamine (**A3**) and 1-methyl-3-[3-(trimethoxysilyl)propyl]imidazolium chloride (**IL1**) the ζ-potential value preceded 40 mV revealing strong positively charged surface and very high stability of colloidal suspension of particles with potential industrial application. It has to be stressed that all ζ-potential measurements were carried out at pH 8.0[70], therefore change in the values can only be a result of successful surface modification.

In order to even further assess the functionalization rate of ZnO surface, elemental analysis using ICP-OES was carried out measuring the molar ratio between Zn and Si in prepared functionalised ZnO systems. The results listed in Table 1 reveal relatively high molar percentage of Si with the values between 11 and 15 % and **AD** with over 17 % Si content. The latter came as no surprise as **AD**-modification underwent self-condensation.

***Table 1**: Material characterisation, antimicrobial activity and leaching of Zn and Si into growth media of pure and functionalized ZnO.*

Sample	Size (DLS) [nm]	ζ-potential [mV]	Si content [%]	Solubility in LB	
				Zn [mgL^{-1}]	Si [mgL^{-1}]
ZnO	77±28	-37.0	0*	0.108	0*
A1	119±34	5.1	15.1	0.012	0.072
A2	79±23	31.6	13.9	0.030	0*
A3	88±24	42.0	14.9	0.034	0*
AD	131±49	6.7	17	0.200	0.011
IL1	79±23	43.4	11.3	0*	0*
IL2	76±21	30.3	13.1	0.006	0.019
C	117±42	5.5	13.2	0*	0.021

* below detection limit

Figures 1SI (supporting information) and 2SI respectfully depict *E. coli* and *S. aureus* growth curves for unmodified and functionalised nanocrystalline ZnO. As previously mentioned it was our goal to produce highly antimicrobial ZnO nanocrystals before any further modification. The antimicrobial activity was determined by calculating minimal inhibitory concentration (Table 2) from Sigmoidal-Boltzmann fitted (non-linear regression) OD_{600} values of growth curves after 12 h (taking into an account 90 % growth reduction). Several concentrations of unmodified ZnO were investigated and the results showed that concentration 0.125 g L^{-1} diminished the bacterial growth by approximately 50 %. This result is comparable with colloidal ZnO[61]. Concentrations of ZnO ≥ 0.25 g L^{-1} inhibited growth of both bacteria strains completely, proving that a very effective antimicrobial precursor material was obtained. It can also be observed that when present in small concentration i.e. 0.0625 g $L^{-1}$of ZnO there was an increased growth rate in the case of *S. aureus* likely caused by a small % of bacteria in the initial culture dying and the dead cells then serving as a food source for the surviving bacteria which can then grow to a higher OD than in the control. **A1**-modified nanocrystalline ZnO revealed decrease of MIC from 0.19 g L^{-1} for pristine ZnO to 0.08 g L^{-1} for *E. coli* and a small decrease of MICfor *S. aureus* (0.12 g L^{-1} compared to 0.13 for ZnO) at the concentration 0.0625 g L^{-1}. This information together with growth curves (Figures 1SI and 2SI) demonstrate very good antimicrobial potential surpassing the previously reported aminopropyltrimethoxysilane-ZnO hybrid[53], where antimicrobial activity against *E. coli* was determined after UV-illumination, by an order of magnitude. N-(2-aminoethyl)-3-aminopropyltrimethoxysilane (**A2**) modified ZnO revealed similar MIC to **A1** for *E. coli* (0.11 g L^{-1})and 0.13 g L^{-1} for *S. aureus*. 3-Methoxysilylpropyldietilenetriamine (**A3**)-modified ZnO was very efficient and both bacteria showing very low MIC values 0.09 g L^{-1} for *E. coli* and 0.11 g L^{-1} for *S. aureus* . **AD**-modification revealed inferior antimicrobial effectiveness

compared to abovementioned amines. This could be explained with the sterical hindrance of two silane groups that also acted as coupling agents consequently causing agglomeration of ZnO particles. MIC values increased compared to ZnO. It is entirely possible that in this case ZnO played the main antimicrobial role and the **AD**-modification caused a slight deterioration of antimicrobial effect. Both selected ionic liquid modifications displayed expected high antimicrobial effectiveness exhibiting low MIC values. In order to assess the antimicrobial quality of modifications examined thus far we replicated the ZnO modification protocol with commercially available silane antimicrobial agent octadecyldimethyl(3-trimethoxysilylpropyl) ammonium chloride (**C**)[71,72] often chosen as a strong antimicrobial textile finishing agent taking advantage of its sol-gel capabilities to covalently bond onto OH groups of the cellulose fibres. In our case it seems that this modification blocked the ZnO surface, caused agglomeration and increased size (according to SEM and DLS) of the particles and subsequently showed impaired antimicrobial activity.

Table 2: Minimal inhibitory concentrations of ZnO and its modifications for *E. coli* and *S. aureus*.

bacteria	MIC (g/L)							
	ZnO	**A1**	**A2**	**A3**	**AD**	**IL1**	**IL2**	**C**
E. coli	0.19±0.00	0.08±0.02	0.11±0.00	0.09±0.02	0.22±0.00	0.10±0.00	0.07±0.01	0.21±0.02
S. aureus	0.13±0.00	0.12±0.00	0.13±0.00	0.11±0.01	0.24±0.01	0.09±0.02	0.10±0.01	0.43±0.05

Several experiments were performed in order to obtain better understanding of the mechanisms responsible for the excellent antimicrobial properties of the investigated materials. Although the optical density measurements of bacterial growth were carried out at 600 nm, therefore relatively far from ZnO's bangap, formation of reactive oxygen species (ROS) cannot be completely overruled, especially, since their existence has been observed also under normal visible light conditions[43]. However, in our opinion this is not the predominant disruptive mechanism in our case. Another possibility would be the release of Zn^{2+} by surface dissolution of ZnO in LB medium. If silane-modified nanomaterials would partially dissolve an increase of Si in the solution would also occur. The results gathered in Table 1 show only a minimal increase (0 – 0.2 mg L^{-1}) of Zn^{2+} and (0 – 0.02 mg L^{-1}) Si compared to LB medium. Antimicrobial activity (Figure 3SI) and minimal inhibitory concentration (MIC) studies were performed also for Zn^{2+} and silanes used for modification of ZnO. The results listed in Table 3 display strong antimicrobial activity of Zn^{2+} with MIC at 0.1 g L^{-1} and relatively weak activities of employed silanes. Reusability studies were also carried out by adding fresh inoculums every 12 h for 5 days. Results gathered in Figure 4SI show excellent antimicrobial long-term efficiency of most of examined materials.

The morphology of *E. coli* before and after treatment reveals significant changes. Figure 5SI unveils considerable damage to bacteria's membrane after 12 h treatment with A3 (0.5 g L^{-1}).

Plate assay was performed to asses killing or inhibition of microorganisms. The results depicted in Figure 6 show 100 % bacterial growth reduction after treatment with A1, A2, A3, IL1 and IL2 using 0.25 and 0.5 g L^{-1} of investigated ZnO materials. ZnO exhibits excellent growth inhibition (<100 CFU mL^{-1}). AD and C modifications on the other hand reveal poor growth inhibition. Confocal fluorescent microscope analysis was performed to assess Live/Dead assay. The results gathered in Figure 6SI depict the ratio between live and dead E. coli bacteria after treatment with 0.125 g L^{-1} of investigated ZnO materials. These results confirm the plate assay.

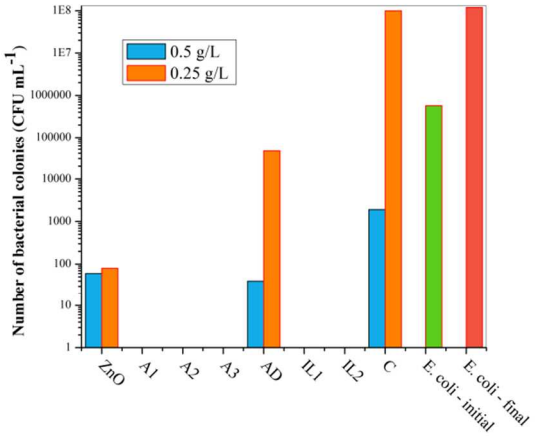

Figure 6: Plate assay for different ZnO modifications

Since the solubility of investigated ZnO materials (measured Zn^{2+} in LB medium) is approximately 500 times lower than the measured MIC of Zn^{2+} we can exclude the release of Zn^{2+} as the predominant mechanism of bacterial inactivation. Moreover, high MIC values of free silanes employed in the study confirm the synergy effect of the functional silanes anchored onto the ZnO surface, causing fatal bacterial membrane disorganization on contact.

Table 4: Minimal inhibitory concentration of Zn^{2+} and functional silanes for *E. coli*.

	MIC (g/L)							
	Zn^{2+}	**A1'**	**A2'**	**A3'**	**AD'**	**IL1'**	**IL2'**	**C'**
E. coli	0.11±0.00	3.9±0.0	6.8±0.2	1.9±0.3	/	62.6±0.1	249±3	/

Conclusions

Synthesis of nanocrystalline ZnO with strong antimicrobial properties was developed and optimised. Its antimicrobial activity was further enhanced by covalent surface modification with functional silanes. Commercially available aminosilanes and especially laboratory-prepared ionic liquid-silanes were successfully attached to the ZnO surface for the first time. Surface alterations were corroborated with TEM and SEM analysis, ζ-potential, IR spectroscopy and elemental composition. These modifications predominantly exhibited significantly improved antimicrobial activity compared to inherently strong activity of prepared ZnO. Amino- and IL-functionalisations of ZnO yielded well-separated particles with an exceptional antimicrobial activity, displaying 100 % bacterial inactivation at merely 0.125 g L^{-1}, enhancing this characteristic for an order of magnitude compared to previously reported results.

Acknowledgements

The authors gratefully acknowledge the financial support from Slovene research agency (Programs P1-0030 and P1-0034). Authors are also indebted to Jerneja Godnjavec for help with the ζ-potential measurements and Bojan Budič for elemental analysis. Authors would like to thank Prof. Dr. Damjana Drobne, Dr. Sara Novak and Tea Romih, Department of Biology, Biotechnical Faculty UL for assistance with bioimaging. Authors are also indebted to Dr. Mojca Benčina and Dr. Iva Hafner and colleagues from Laboratory L-11 for providing fluorescent microscopy and assisting bacterial growth experiments.

References

[a] National Institute of Chemistry, Hajdrihova 19, SI-1000 Ljubljana, Slovenia
[b] Jožef Stefan Institute, Jamova cesta 39, SI-1000 Ljubljana, Slovenia
* Emails: vasko.jovanovski@ki.si, zorica.crnjak.orel@ki.si

Electronic Supplementary Information (ESI) available: [details of any supplementary information available should be included here]. See DOI: 10.1039/b000000x/

1. A. McLaren, T. Valdes-Solis, G. Li and S. C. Tsang, J. Am. Chem. Soc., 2009, 131, 12540-12541.
2. E. S. Jang, J. H. Won, S. J. Hwang and J. H. Choy, Adv. Mater., 2006, 18, 3309-3312.
3. K. S. Leschkies, R. Divakar, J. Basu, E. Enache-Pommer, J. E. Boercker, C. B. Carter, U. R. Kortshagen, D. J. Norris and E. S. Aydil, Nano Lett., 2007, 7, 1793-1798.
4. Q. Zhang, C. S. Dandeneau, X. Zhou and C. Cao, Adv. Mater., 2009, 21, 4087-4108.
5. J. Zhang, S. Wang, M. Xu, Y. Wang, B. Zhu, S. Zhang, W. Huang and S. Wu, Cryst. Growth Des., 2009, 9, 3532-3537.
6. A. Menzel, K. Subannajui, F. Güder, D. Moser, O. Paul and M. Zacharias, Adv. Funct. Mater., 2011, 21, 4342-4348.
7. A. Sinhamahapatra, A. K. Giri, P. Pal, S. K. Pahari, H. C. Bajaj and A. B. Panda, J. Mater. Chem., 2012, 22, 17227-17235.
8. G. Zhu, R. Yang, S. Wang and Z. L. Wang, Nano Lett., 2010, 10, 3151-3155.
9. X. W. Sun and J. X. Wang, Nano Lett., 2008, 8, 1884-1889.
10. A. Becheri, M. Dürr, P. Lo Nostro and P. Baglioni, J. Nanopart. Res., 2008, 10, 679-689.
11. K. Senthilkumar, O. Senthilkumar, K. Yamauchi, M. Sato, S. Morito, T. Ohba, M. Nakamura and Y. Fujita, Phys. Status Solidi B, 2009, 246, 885-888.
12. S. Liang, K. Xiao, Y. Mo and X. Huang, J. Membrane Sci., 2012, 394-395, 184-192.
13. Q. Li, S. Mahendra, D. Y. Lyon, L. Brunet, M. V. Liga, D. Li and P. J. J. Alvarez, Water Res., 2008, 42, 4591-4602.
14. C. G. Allen, D. J. Baker, J. M. Albin, H. E. Oertli, D. T. Gillaspie, D. C. Olson, T. E. Furtak and R. T. Collins, Langmuir, 2008, 24, 13393-13398.
15. C. D. Corso, A. Dickherber and W. D. Hunt, Biosens. Bioelectron., 2008, 24, 805-811.
16. S. A. Haque, S. Koops, N. Tokmoldin, J. R. Durrant, J. Huang, D. D. C. Bradley and E. Palomares, Adv. Mater., 2007, 19, 683-687.
17. M. Abbasian, N. K. Aali and S. E. Shoja, J. Macromol. Sci. A, 2013, 50, 966-975.
18. C. Bressy, V. G. Ngo, F. Ziarelli and A. Margaillan, Langmuir, 2012, 28, 3290-3297.
19. F. Grasset, N. Saito, D. Li, D. Park, I. Sakaguchi, N. Ohashi, H. Haneda, T. Roisnel, S. Mornet and E. Duguet, J. Alloys Compd., 2003, 360, 298-311.
20. C. Badre and T. Pauporté, Adv. Mater., 2009, 21, 697-701.
21. C. Badre, T. Pauporté, M. Turmine and D. Lincot, Superlattices Microstruct., 2007, 42, 99-102.
22. M. Li, J. Zhai, H. Liu, Y. Song, L. Jiang and D. Zhu, J. Phys. Chem. B, 2003, 107, 9954-9957.
23. Y. Li, W. Cai, G. Duan, B. Cao, F. Sun and F. Lu, J. Colloid Interface Sci., 2005, 287, 634-639.
24. R. Y. Hong, J. Z. Qian and J. X. Cao, Powder Technol., 2006, 163, 160-168.
25. L. a. SelegÅrd, V. Khranovskyy, F. Söderlind, C. Vahlberg, M. Ahrén, P.-O. Käll, R. Yakimova and K. Uvdal, ACS Appl. Mater. Interfaces, 2010, 2, 2128-2135.
26. J. Zeng, H. Liu, J. Chen, J. Huang, J. Yu, Y. Wang and X. Chen, Analyst, 2012, 137, 4295-4301.
27. V. Jovanovski, V. González-Pedro, S. Giménez, E. Azaceta, G. Cabañero, H. Grande, R. Tena-Zaera, I. Mora-Seró and J. Bisquert, J. Am. Chem. Soc., 2011, 133, 20156-20159.
28. A. Brazier, G. B. Appetecchi, S. Passerini, A. Surca Vuk, B. Orel, F. Donsanti and F. Decker, Electrochim. Acta, 2007, 52, 4792-4797.
29. A. Balducci, S. S. Jeong, G. T. Kim, S. Passerini, M. Winter, M. Schmuck, G. B. Appetecchi, R. Marcilla, D. Mecerreyes, V. Barsukov, V. Khomenko, I. Cantero, I. De Meatza, M. Holzapfel and N. Tran, J. Power Sources, 2011, 196, 9719-9730.

30. T. Sato, G. Masuda and K. Takagi, Electrochim. Acta, 2004, 49, 3603-3611.
31. J. Yuan, D. Mecerreyes and M. Antonietti, Prog. Polym. Sci., 2013, 38, 1009-1036.
32. G. Quijano, A. Couvert and A. Amrane, Bioresour. Technol., 2010, 101, 8923-8930.
33. J. Y. Dong, Y. J. Hsu, D. S. H. Wong and S. Y. Lu, J. Phys. Chem. C, 2010, 114, 8867-8872.
34. W.-W. Wang and Y.-J. Zhu, Inorg. Chem. Commun., 2004, 7, 1003-1005.
35. J. Wang, J. Cao, B. Fang, P. Lu, S. Deng and H. Wang, Mater. Lett., 2005, 59, 1405-1408.
36. H. Zhu, J.-F. Huang, Z. Pan and S. Dai, Chem. Mater., 2006, 18, 4473-4477.
37. J. C. Tiller, S. B. Lee, K. Lewis and A. M. Klibanov, Biotechnol. Bioeng., 2002, 79, 465-471.
38. A. M. Klibanov, J. Mater. Chem., 2007, 17, 2479-2482.
39. N. M. Milović, J. Wang, K. Lewis and A. M. Klibanov, Biotechnol. Bioeng., 2005, 90, 715-722.
40. G. N. Tew, R. W. Scott, M. L. Klein and W. F. DeGrado, Acc. Chem. Res., 2009, 43, 30-39.
41. K. Page, M. Wilson and I. P. Parkin, J. Mater. Chem., 2009, 19, 3819-3831.
42. L. K. Adams, D. Y. Lyon and P. J. J. Alvarez, Water Res., 2006, 40, 3527-3532.
43. N. Jones, B. Ray, K. T. Ranjit and A. C. Manna, FEMS Microbiol. Lett., 2008, 279, 71-76.
44. A. Lipovsky, Y. Nitzan, A. Gedanken and R. Lubart, Nanotechnology, 2011, 22, 105101.
45. O. Akhavan, R. Azimirad and S. Safa, Mater. Chem. Phys., 2011, 130, 598-602.
46. M. Li, S. Pokhrel, X. Jin, L. Mädler, R. Damoiseaux and E. M. V. Hoek, Environ. Sci. Technol., 2010, 45, 755-761.
47. P. Joshi, S. Chakraborti, P. Chakrabarti, D. Haranath, V. Shanker, Z. A. Ansari, S. P. Singh and V. Gupta, J. Nanosci. Nanotechnol., 2009, 9, 6427-6433.
48. G. Applerot, A. Lipovsky, R. Dror, N. Perkas, Y. Nitzan, R. Lubart and A. Gedanken, Adv. Funct. Mater., 2009, 19, 842-852.
49. K. R. Raghupathi, R. T. Koodali and A. C. Manna, Langmuir, 2011, 27, 4020-4028.
50. Z. Huang, X. Zheng, D. Yan, G. Yin, X. Liao, Y. Kang, Y. Yao, D. Huang and B. Hao, Langmuir, 2008, 24, 4140-4144.
51. H. Yin, P. S. Casey, M. J. McCall and M. Fenech, Langmuir, 2010, 26, 15399-15408.
52. Y. H. Leung, C. M. N. Chan, A. M. C. Ng, H. T. Chan, M. W. L. Chiang, A. B. Djurišić, Y. H. Ng, W. Y. Jim, M. Y. Guo, F. C. C. Leung, W. K. Chan and D. T. W. Au, Nanotechnology, 2012, 23, 475703.
53. P. Thevenot, J. Cho, D. Wavhal, R. B. Timmons and L. Tang, Nanomed. Nanotechnol., 2008, 4, 226-236.
54. P. Gerhardt, Methods for general and molecular bacteriology, Am. Soc. Microbiol., 1994.
55. T. Ghoshal, S. Kar and S. Chaudhuri, Cryst. Growth Des., 2007, 7, 136-141.
56. B. Orel, A. S. Vuk, V. Jovanovski, R. Ješe, L. S. Perše, S. B. Hočevar, E. A. Hutton, B. Ogorevc and A. Jesih, Electrochem. Commun., 2005, 7, 692-696.
57. E. Stathatos, V. Jovanovski, B. Orel, I. Jerman and P. Lianos, J.Phys. Chem. C, 2007, 111, 6528-6532.
58. E. S. Sashina, D. A. Kashirskii, M. Zaborski and S. Jankowski, Russ. J. Gen. Chem., 2012, 82, 1994-1998.
59. R. Brayner, R. Ferrari-Iliou, N. Brivois, S. Djediat, M. F. Benedetti and F. Fiévet, Nano Lett., 2006, 6, 866-870.
60. V. B. Schwartz, F. Thétiot, S. Ritz, S. Pütz, L. Choritz, A. Lappas, R. Förch, K. Landfester and U. Jonas, Adv. Funct. Mater., 2012, 22, 2376-2386.
61. T. Jin, D. Sun, J. Y. Su, H. Zhang and H. J. Sue, J. Food Sci., 2009, 74, M46-M52.
62. M. Bitenc and Z. Crnjak Orel, Mater. Res. Bull., 2009, 44, 381-387.
63. M. Bitenc, P. Podbrščček, P. Dubček, S. Bernstorff, G. Dražić, B. Orel, S. Pejovnik and Z. Crnjak Orel, Chem – A Eur. J., 2010, 16, 11481-11488.
64. A. Anžlovar, Z. Crnjak Orel, K. Kogej and M. Žigon, J. Nanomater., 2012, 2012.
65. F. J. Shan, C. S. Liu, S. H. Wang and G. C. Qi, Acta Metall. Sin. (Eng. Lett.), 2008, 21, 245-252.
66. W. Stählin and H. R. Oswald, J. Solid State Chem., 1971, 3, 252-255.
67. N. Sato, Y. Hamada and M. Tsuboi, Spectrochim. Acta A, 1987, 43, 943-954.
68. E. H. P. Logtenberg and H. N. Stein, J. Colloid Interface Sci., 1986, 109, 190-200.
69. A. J. Isquith, E. A. Abbott and P. A. Walters, Appl. Microbiol., 1972, 24, 859-863.
70. B. Simoncic and B. Tomsic, Tex. Res. J., 2010, 80, 1721-1737.

Amino- and ionic liquid-functionalised nanocrystalline ZnO via silane anchoring - an antimicrobial synergy

Marjeta Čepin[a], Vasko Jovanovski[a]*, Matejka Podlogar[b] and Zorica Crnjak Orel[a]*

[a]National Institute of Chemistry, Hajdrihova 19, SI-1000 Ljubljana, Slovenia
[b]Jožef Stefan Institute, Jamova cesta 39, SI-1000 Ljubljana, Slovenia